



Improving the optical performance of multi-chip LEDs by using patterned phosphor configurations

XINRUI DING,^{1,2} QIU CHEN,¹ YONG TANG,¹ JIASHENG LI,¹ DEEPAK TALWAR,³ BINHAI YU,¹ AND ZONGTAO LI^{1,*}

¹Key Laboratory of Surface Functional Structure Manufacturing, Guangdong, Higher Education Institutes, South China University of Technology, Guangzhou 510641, China

²Department of Mechanical Engineering, University of California at Berkeley, Berkeley, CA 94720-5800 USA

³Clarity Movement Co., Berkeley, CA, 94704, USA

*meztl@scut.edu.cn

Abstract: In order to improve the color uniformity of multi-chip LEDs, a patterned phosphor configuration has been proposed by using pulsing spray process. The patterned phosphor has detached yellow and red phosphor regions matching every single LED chip. Optical performances of different phosphor parameters are experimentally investigated. The results show that the yellow central coating (YCC) configuration produces outstanding performance not only in chromatic uniformity but also in luminous. In comparison with the conventional phosphor coating, the YCC patterned phosphor LED can improve the luminous flux by 20.6%, and decrease the difference of the correlated color temperature (CCT) distribution from 1362K to 489K. We believe that the patterned phosphor configuration can be used for improving optical properties of multi-chip LEDs.

© 2018 Optical Society of America under the terms of the [OSA Open Access Publishing Agreement](#)

OCIS codes: (230.3670) Light-emitting diodes; (260.2160) Energy transfer; (300.6280) Spectroscopy, fluorescence and luminescence; (330.1710) Color, measurement.

References and links

1. D. S. Meygaard, G. B. Lin, J. Cho, and E. F. Schubert, “9 - Efficiency droop in gallium indium nitride (GaInN)/gallium nitride (GaN) LEDs,” in *Nitride Semiconductor Light-Emitting Diodes (LEDs)*, J. Huang, H.-C. Kuo, and S.-C. Shen, eds. (Woodhead Publishing, 2014), pp. 279–300.
2. J. McKittrick and L. E. Shea-Rohwer, “Review: Down Conversion Materials for Solid-State Lighting,” *J. Am. Ceram. Soc.* **97**(5), 1327–1352 (2014).
3. J. Cho, E. F. Schubert, and J. K. Kim, “Efficiency droop in light-emitting diodes: Challenges and countermeasures,” *Laser Photonics Rev.* **7**, 408–421 (2012).
4. C. EZ-1950-P, [“http://www.cree.com/led-chips/products/ez-p-leds/ez1950-p”](http://www.cree.com/led-chips/products/ez-p-leds/ez1950-p) (2015).
5. Y. Peng, R. Li, H. Cheng, Z. Chen, H. Li, and M. Chen, “Facile preparation of patterned phosphor-in-glass with excellent luminous properties through screen-printing for high-power white light-emitting diodes,” *J. Alloys Compd.* **693**, 279–284 (2017).
6. C.-H. Chiang, H.-Y. Tsai, T.-S. Zhan, H.-Y. Lin, Y.-C. Fang, and S.-Y. Chu, “Effects of phosphor distribution and step-index remote configuration on the performance of white light-emitting diodes,” *Opt. Lett.* **40**(12), 2830–2833 (2015).
7. X. Ding, J. Li, Q. Chen, Y. Tang, Z. Li, and B. Yu, “Improving LED CCT uniformity using micropatterned films optimized by combining ray tracing and FDTD methods,” *Opt. Express* **23**(3), A180–A191 (2015).
8. Y. Tang, G. Liang, J. Chen, S. Yu, Z. Li, L. Rao, and B. Yu, “Highly reflective nanofiber films based on electrospinning and their application on color uniformity and luminous efficacy improvement of white light-emitting diodes,” *Opt. Express* **25**(17), 20598–20611 (2017).
9. H. Xiao, Y.-J. Lu, Z.-Q. Guo, Y. Lin, T.-M. Shih, and Z. Chen, “Improvements on optical and chromatic uniformities of light-emitting diodes with microscale-roughness-controlled surfaces,” *IEEE Photonics J.* **7**, 1–8 (2015).
10. J. K. Kim, H. Luo, E. F. Schubert, J. Cho, C. Sone, and Y. Park, “Strongly enhanced phosphor efficiency in GaInN white light-emitting diodes using remote phosphor configuration and diffuse reflector cup,” *Jpn. J. Appl. Phys.* **44**(21), L649–L651 (2005).

11. L. Jia-Sheng, C. Jia-Xiao, L. Li-Wei, L. Zong-Tao, T. Yong, Y. Bin-Hai, and D. Xin-Rui, "A Detailed Study on Phosphor-Converted Light-Emitting Diodes With Multi-Phosphor Configuration Using the Finite-Difference Time-Domain and Ray-Tracing Methods," *IEEE J. Quantum Electron.* **51**, 1–10 (2015).
12. L. Rao, Y. Tang, Z. Li, X. Ding, J. Li, S. Yu, C. Yan, and H. Lu, "Effect of ZnO nanostructures on the optical properties of white light-emitting diodes," *Opt. Express* **25**(8), A432–A443 (2017).
13. J. Li, Z. Li, Z. Li, Y. Tang, X. Ding, and B. Yu, "Improvement in optical performance and color uniformity by optimizing the remote phosphor caps geometry for chip-on-board light emitting diodes," *Solid-State Electron.* **126**, 36–45 (2016).
14. J. Li, Z. Li, G. Liang, S. Yu, Y. Tang, and X. Ding, "Color uniformity enhancement for COB WLEDs using a remote phosphor film with two freeform surfaces," *Opt. Express* **24**(21), 23685–23696 (2016).
15. T. Pai-Yang, H. Hou-Kuei, S. Jian-Min, K. Ming-Chi, and W. Yeong-Her, "High Thermal Stability and Wide Angle of White Light Chip-on-Board Package Using a Remote Phosphor Structure," *IEEE Electron Device Lett.* **36**(3), 250–252 (2015).
16. S. Wang, X. Chen, M. Chen, H. Zheng, H. Yang, and S. Liu, "Improvement in angular color uniformity of white light-emitting diodes using screen-printed multilayer phosphor-in-glass," *Appl. Opt.* **53**(36), 8492–8498 (2014).
17. Z.-Y. Liu, C. Li, B.-H. Yu, Y.-H. Wang, and H.-B. Niu, "Uniform white emission of WLEDs realized by multilayer phosphor with pyramidal shape and inverted concentration distribution," *IEEE Photonics Technol. Lett.* **24**(17), 1558–1560 (2012).
18. M.-T. Lin, S.-P. Ying, M.-Y. Lin, K.-Y. Tai, S.-C. Tai, C.-H. Liu, J.-C. Chen, and C.-C. Sun, "Ring remote phosphor structure for phosphor-converted white LEDs," *IEEE Photonics Technol. Lett.* **22**(8), 574–576 (2010).
19. M.-T. Lin, S.-P. Ying, M.-Y. Lin, K.-Y. Tai, S. Tai, C.-H. Liu, J.-C. Chen, and C.-C. Sun, "Design of the Ring Remote Phosphor Structure for Phosphor-Converted White-Light-Emitting Diodes," *Jpn. J. Appl. Phys.* **49**(7), 072101 (2010).
20. J.-S. Li, Y.-H. Chen, Z.-T. Li, S.-D. Yu, Y. Tang, X.-R. Ding, and W. Yuan, "ACU Optimization of pcLEDs by combining the pulsed spray and feedback method," *J. Disp. Technol.* **12**(10), 1229–1234 (2016).
21. Z.-T. Li, Y. Tang, Z.-Y. Liu, Y.-E. Tan, and B.-M. Zhu, "Detailed study on pulse-sprayed conformal phosphor configurations for LEDs," *J. Disp. Technol.* **9**(6), 433–440 (2013).
22. Y. Peng, X. Guo, R. Li, H. Cheng, and M. Chen, "Thermally stable WLEDs with excellent luminous properties by screen-printing a patterned phosphor glass layer on a microstructured glass plate," *Appl. Opt.* **56**(12), 3270–3276 (2017).
23. S.-P. Ying and H.-Y. Chien, "Effect of reassembled remote phosphor geometry on the luminous efficiency and spectra of white light-emitting diodes with excellent color rendering property," *IEEE Trans. Electron Dev.* **63**(3), 1117–1121 (2016).
24. J. S. Lee, P. Arunkumar, S. Kim, I. J. Lee, H. Lee, and W. B. Im, "Smart design to resolve spectral overlapping of phosphor-in-glass for high-powered remote-type white light-emitting devices," *Opt. Lett.* **39**(4), 762–765 (2014).
25. Q. Chen, Z. Li, K. Chen, Y. Tang, X. Ding, and B. Yu, "CCT-tunable LED device with excellent ACU by using micro-structure array film," *Opt. Express* **24**(15), 16695–16704 (2016).

1. Introduction

White light emitting diode (WLED) with blue-chip coated with phosphor has been widely used for general lighting, display, and communication [1, 2]. This innovation played a major role in accelerating the illumination revolution. After more than two decades of development, the quality of the WLED has been greatly enhanced on their efficiency, lifetime, and consistency. However, there are some limitations that need to be addressed, such as limited efficiency of phosphor and lack of color uniformity [3]. The GaN-based blue WLEDs are fabricated on a sapphire (Al_2O_3), silicon (Si) or carborundum (SiC) wafer using epitaxy method by metal organic chemical vapor deposition (MOCVD). The LED wafers need to be cut into small dies and classified into different bins for the application. Even though the highest commercial power for a single LED chip can reach over 10W from CREE[®] EZ1950-P [4], it is still insufficient for high-power applications. Multi-chip LED package with chip on board (COB) technology is a preferable solution for high power applications.

In conventional multi-chip LEDs, a multi-color phosphor is usually blended with the silicone and coated around the LED chips. The scattering and absorption of the phosphor particles limit the phosphor conversion efficiency [5, 6]. Color uniformity is another important quality index of the WLED. Since the white light is the combination of short wavelength light from the WLED chip and long wavelength light from the phosphor, the mixture of different colors is difficult to be made uniform [7].

In order to solve the above issues, some approaches have been developed. One solution is to enhance the surface scattering to uniformly mix the color, such as using an electrospinning

nano-fiber scattering enhanced film [8], micropatterned array optical structures [7] and micro-scale roughness controlled surfaces [9, 10]. Another solution is to improve the particle scattering performance. In our previous work, we studied the particle scattering property using the particle shape through the finite difference time domain (FDTD) and ray tracing (RT) methods [11]. The results showed that the particle shape had a significant impact on the performance. Subsequently, we used different shapes of ZnO nanoparticles to improve the rescattering performance in order to enhance the angular color uniformity (ACU) [12]. However, strong scattering usually comes with strong absorption, which decreases the luminous efficiency. Therefore, various phosphor structures have been produced, such as remote phosphor cap [13–15], pyramidal remote phosphor layer [16, 17], ring-shaped remote phosphor layer [18, 19] and freeform phosphor layer [20]. Z.T. Li's group proposed a multilayer phosphor conformal structure with the red phosphor layer on the bottom and the yellow phosphor layer on the top. This interesting concept for fabricating a low correlated color temperature (CCT) and high color rendering index (CRI) WLED device not only decreases the dosage of high-cost nitride phosphor but also results in good CCT uniformity [21]. Nevertheless, there is a large spectral overlap between the yellow emitted spectrum and the red excited spectrum. Patterned phosphor structure is one of the best solutions to solve this problem. Some researchers developed a screen printing method to prepare a phosphor-in-glass remote phosphor plate with some rotational symmetry patterns for improving the color uniformity [5, 22–24]. Chen et al. developed a color tunable multi-chip LED by using double rings shaped phosphor structure [25]. However, the above researchers did not consider the matching between the patterned phosphor structures and emitting distribution of every single LED chip, which limited the chromatic performance of the patterned phosphor structures. In this work, a patterned phosphor configuration by using pulsing spray process has been studied to characterize the color uniformity of multi-chip LEDs, which is expected to improve optical properties of multi-chip LEDs.

2. Experimental setups

A commercial P2828 multichip LED from Nationstar[®] was selected for this work. It contains 25 blue LED chips with a chip size of 43 μm *89 μm , a peak wavelength of 455nm and 5-series, 5-parallel wire bonding connections. Yellow YAG: Ce phosphor (type: YAG04 from Intematix[®]) and red nitride phosphor (type: 0764 from Grinm[®]) were selected for converting blue light to yellow light and red light, respectively. The weight ratio of the red and yellow phosphor is 0.284:1.000. The total phosphor weight on each sample is controlled to be 45.00 \pm 0.01mg through pulse spraying equipment. The fabrication process is demonstrated in Fig. 1(a). 1) The multichip LED was covered with transparent silicone after the die bonding and wire bonding process. The dam decides the distance between the phosphor layer and the top of the LED chip, which is represented by H as shown in Fig. 2. The dam is controlled by the distance between the syringe needle and the LED base plate through a high precision dispensing machine (Musashi 300DS). In this work, we chose 0.42mm, 0.54mm and 0.66mm three distances as comparisons. 2) Three masks as shown in Fig. 1(b) were applied to carry out the phosphor spraying process. The mask A has 25 square holes with five different side lengths (0.9mm, 1.2mm, 1.5mm, 1.8mm, 2.1mm, 2.4mm) and spatial period of 3mm, same as the spatial period of the LED chips. After the first spraying round through mask A, 25 square phosphor islands were coated on the silicone surface. 3) Mask B for the second spraying round covered the 25 square phosphor islands and allowed the other phosphor to be coated in the surrounding areas. 4) Mask C for the third spraying round covered the already sprayed area and exposed the remaining area without the coating. After the third round spraying, the whole surface of the COB was coated with phosphors without any overlap. Finally, the devices were baked for 2 hours at 150°C.

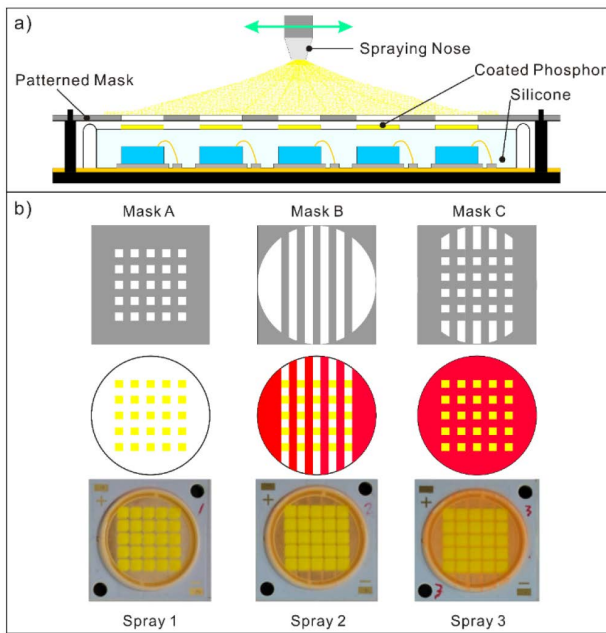


Fig. 1. The fabricating process of the patterned phosphor multi-chip LED, (a) the cross-section view of the LED structure, (b) three spraying process with three matched masks.

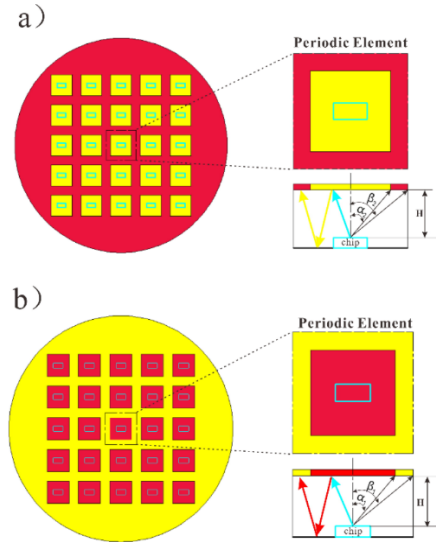


Fig. 2. Two configurations of patterned phosphor, (a) yellow central coating (YCC), and (b) red central coating.

There are two configurations for the red and yellow patterned phosphor as shown in Fig. 2. One configuration is named as the yellow central coating (YCC) and the other one is named as the red central coating (RCC). The phosphor mass on each sample was kept constant by measuring the area of each color, and the weight of the phosphor and silicon before each spray process. The sprayed material on each multi-chip LED includes 1.72mg red nitride phosphor, 6.04mg yellow YAG phosphor, and 11.09mg silicone.

The measurement system (Instrument system[®]) includes a 0.5m integrating sphere, a spectrometer, a Keithley[®] 2420 DC adjustable source and a computer for data collection. To reduce the thermal effect from the LED chips, a cold plate with temperature controller was applied in this work. The plate temperature was kept at $25 \pm 0.5^\circ\text{C}$ during the measurement.

3. Results and discussion

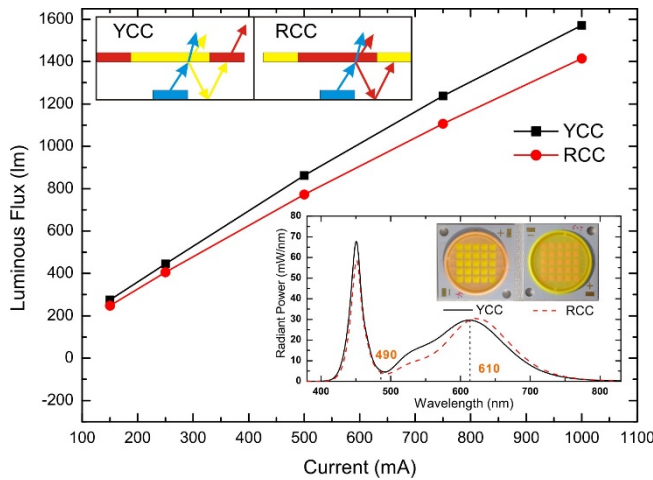


Fig. 3. The luminous flux of YCC and RCC LEDs at different input currents.

Luminous flux is an important property of multi-chip LEDs. The sample with the side length of 2.1mm of the phosphor island and 0.54mm silicone thickness was chosen to contrast the YCC and RCC phosphor configurations. Figure 3 shows the luminous flux of the YCC and the RCC LEDs at different currents. The luminous flux curves increase linearly with input current, which indicates the non-radiative recombination is not serious under the current of 1000mA. The luminous flux of the YCC type of the phosphor configuration is higher than the RCC type. The average improvement is 11.1%. At the current of 1000mA, the luminous fluxes of the YCC and RCC LED are 1571.4lm and 1414.4lm, respectively. Intuitively, this is the consequence of the fact that yellow phosphor can converse more blue light than the red phosphor. The Lambertian distribution of the blue light from the LED chip is mainly concentrated on the top of the LED chip. Therefore, the central yellow phosphor will convert most of the blue light down to the green and yellow light, which is more sensitive to the human eyes. In the inserted spectrum plot of Fig. 3 (right bottom corner), the radiant power of the YCC LED from 490nm to 610nm is higher than that of the RCC LED, and it is lower than the RCC LED in the range of 610nm to 780nm. Interestingly, the two types of the phosphor configurations have the similar correlative color temperatures (CCT). At the current of 1000mA, the CCTs of the YCC and the RCC are 4875K and 4853K, respectively. Although the red phosphor in the RCC configuration converts most of the blue light down to red light (above 620nm), the radiant power from 610nm of the RCC LED is lightly higher than that of the YCC LED. One possible explanation for this is the spectral overlap, which implies the red phosphor in the YCC LED can re-absorb and re-emit the back-scattering yellow light from the central yellow phosphor [11], and can convert the yellow light down to red light. While in the RCC LED, the back-scattered red light is still re-absorbed by the surrounding yellow phosphor, however, it is not re-emitted as the yellow light. The schematic diagram is inserted in Fig. 3 (left top corner). Even though the spectral overlap still exists, it is weaker than the conventional mixture or multi-layer phosphor structures. It can be seen that the YCC configuration is better than the RCC configuration on luminous flux at the same CCT value. Therefore, in the following discussion, we will focus on the YCC configuration.

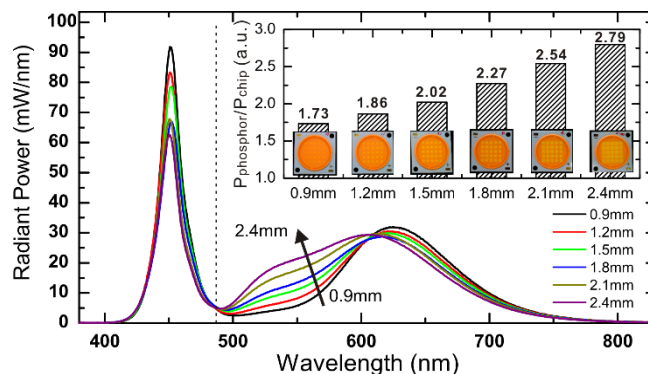


Fig. 4. The spectra of different phosphor island side length, the insert is the $P_{\text{phosphor}}/P_{\text{chip}}$ ratio of different phosphor island side length

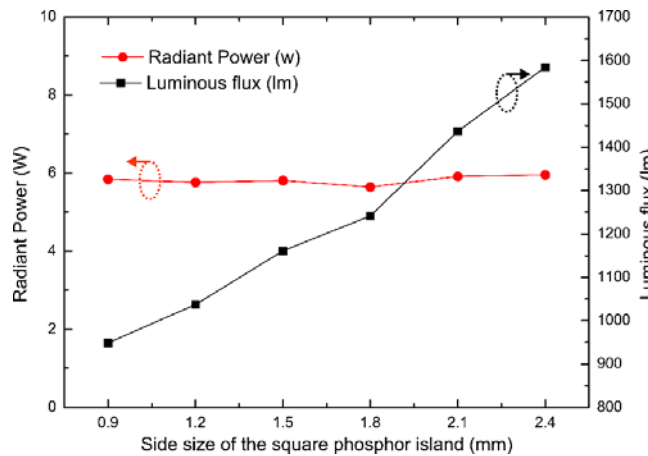


Fig. 5. The radiant power (left) and luminous flux (right) of different side length phosphor islands

Figure 4 shows the spectrum of the YCC multi-chip LEDs with different side lengths of the 25 square YAG phosphor islands. The measurement current is 1000mA. According to the spectrums, it can be divided into three wavebands: blue emission (380-490nm), yellow and green emission (490nm-610nm) and red emission (above 610nm). As can be seen from Fig. 4, the blue emission is decreased with the increase of the side length. This variation means that the phosphor is not saturated. For the yellow and green emission, the power increases with the increasing side length of the YAG phosphor island. The emission of the red light with a side length of the YAG phosphor island varies inversely to that of the yellow and green emission, but the variation in the red emission is less than in the yellow and green emission. Here, the spectrum is divided into two parts at 490nm (black dash line). The radiant power of wavelength less than 490nm is defined as P_{chip} , and the radiant power of wavelength larger than 490nm is defined as P_{phosphor} . The ratios of $P_{\text{phosphor}}/P_{\text{chip}}$ of different phosphor island side length are shown in the inserted diagram in Fig. 4. The results indicate that the conversion ratio of the large phosphor area is higher than that of the small phosphor area. The main reason leading to this results is that the Lambertian blue emission converges mostly to the center of the structure. More blue emission can be converted into yellow-green light with large YAG phosphor area. Moreover, since the red and yellow phosphor ratio and total phosphor weight are the same, the sample with a small side length of the YAG phosphor island has a thick YAG phosphor layer and a thin Nitride phosphor layer. Even though the thicker phosphor helps in improving the conversion of the yellow phosphor under unsaturated

conditions, the spectral results also imply that the area of the phosphor is the dominant factor affecting the conversion compared with the phosphor thickness.

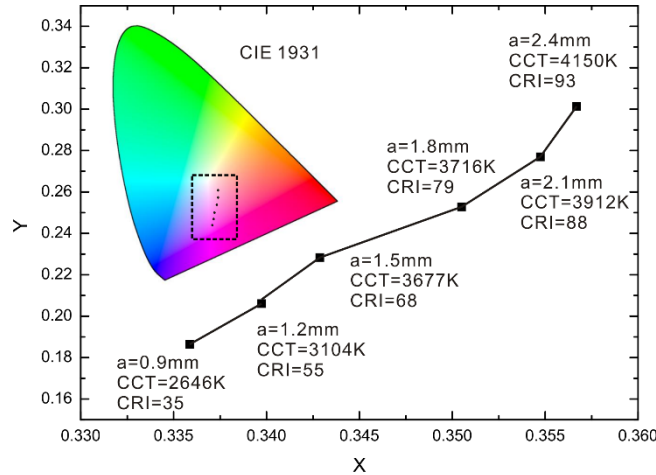


Fig. 6. The chromatic coordinates of different phosphor island side lengths on the CIE1931 chromatic map

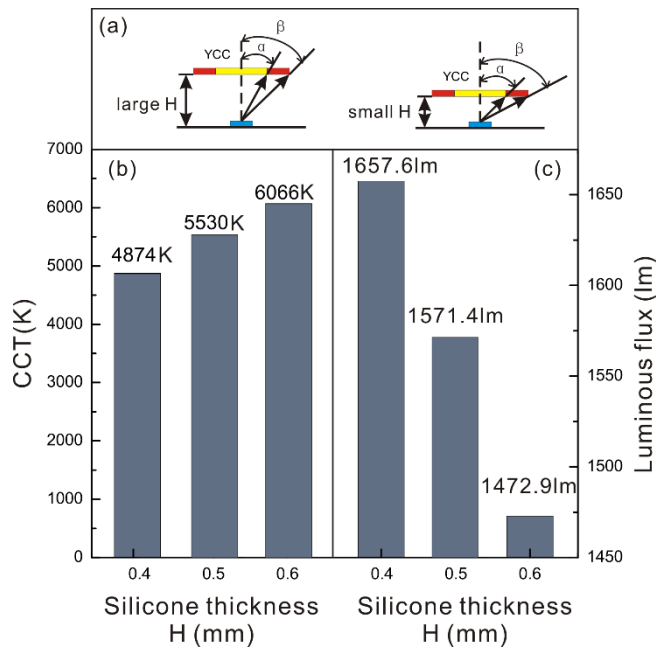


Fig. 7. Luminous fluxes and CCT values of three different silicone thicknesses (H). (a) the schematic diagram about rays emitted at different H, (b) the CCTs and (c) the luminous flux at different H

Figure 5 displays the radiant power and luminous flux of the YCC LED with different YAG phosphor island side lengths. The radiant power varies slightly with different yellow phosphor side lengths at an average power of 5.8W. However, the luminous fluxes increase with the YAG phosphor island side lengths significantly. The reason is that at the same power level, the more human sensitive emission is converted by the phosphor with large phosphor island side lengths than that converted by smaller YAG phosphor island side lengths. The chromatic coordinates of different phosphor island side lengths on the CIE1931 chromatic

map are shown in Fig. 6. With the increasing YAG phosphor island side length, the color shifts from blue to yellow, in addition, the color rendering index (CRI) increases from 35 to 93. Generally, the LED light with CCT from 3000K to 6000K and CRI above 70 is suitable for lighting applications. Therefore, in this work, the optimal side length of the square phosphor island should be larger than 1.8mm. Observing from another side, by changing the patterned size of the mask, the CCT and CRI can be adjusted. It is convenient for the industry because it is not necessary to prepare different red and yellow ratio phosphors when producing different CCT or CRI products.

The thickness of the silicone is another parameter that can affect the properties of the patterned phosphor. Three thicknesses, 0.42mm, 0.54mm, and 0.66mm, were selected in this work to investigate the influence of the silicone thickness. Figures 7(b) and 7(c) shows the CCTs and luminous fluxes of different silicone thicknesses at 1000mA. The CCT values of the thickness of 0.42mm, 0.54mm, and 0.66mm are 4874K, 5530K and 6066K, respectively. It demonstrates that more phosphor is stimulated when the phosphor layer is close to the LED chip. The luminous fluxes of the patterned phosphor with silicone thickness of 0.42mm, 0.54mm, and 0.66mm are 1657.6lm, 1571.4lm, and 1472.9lm, respectively. When the phosphor is close to the LED chip, the vertex angles (α for YAG, β for Nitride, the schematic diagram is shown in Fig. 7 (a)) increase, thereby, more phosphor is stimulated, which increases the luminous flux of the LED.

Further, the YCC and RCC patterned phosphor LED, conventional mixed phosphor and remote phosphor configurations are compared to investigate their optical characteristics. For the conventional mixed phosphor LED, the red and yellow phosphor was uniformly mixed with silicone and coated onto the LED chips. For the remote phosphor LED, the red and yellow phosphor was sprayed on to the transparent silicone layer. Both of the conventional and remote phosphor configurations have the same total phosphor weight and the weight ratio of red and yellow phosphor as YCC and RCC LEDs. The schematic diagram of the four LEDs is shown in the bottom of Fig. 8. The luminous fluxes at 1000mA of YCC, RCC, conventional and remote phosphor samples are shown in Fig. 8. The YCC configuration performs the best luminous property with a luminous flux of 1571.4lm. The luminous flux produced by the RCC configuration is worse than that of the remote phosphor configuration. At 1000mA, the luminous flux produced by the remote phosphor LED 1478.0lm whereas the luminous flux produced by the RCC phosphor LED is 1414.4lm. The conventional configuration showed the worst luminous performance with the production of 1303.0lm of luminous flux at 1000mA. The result indicates that the luminous flux can be improved approximately 20.6% by applying YCC patterned phosphor.

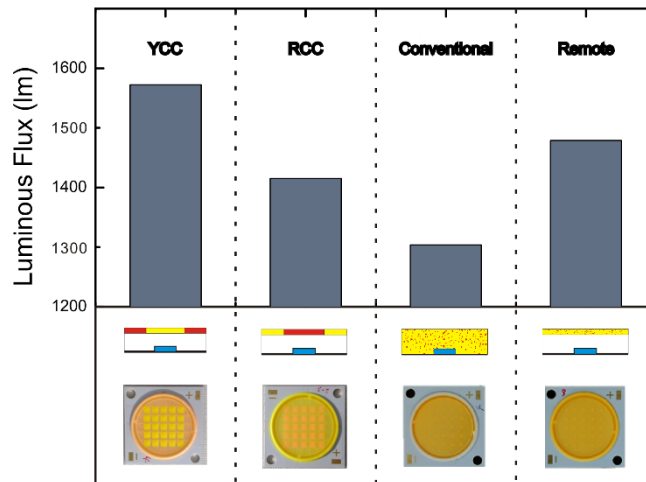


Fig. 8. The luminous flux of four types of multi-chip LEDs

The distribution of the CCT and normalized intensity are shown in Fig. 9 and Fig. 10, respectively. Among the three CCT distributions, the highest CCT values appear in the center of the LEDs, and the CCT values decrease with the increasing vertex angles. Similar distributions can be observed in the normalized intensity as well. The largest CCT differences of the conventional, remote phosphor and YCC configuration are 1362K, 3257K and 489K, respectively. The YCC configuration illustrates the best CCT uniformity with average CCT value of 4251K. The average CCT of the remote and conventional phosphor configuration are 6535K and 5369K, respectively. The CCT value of the YCC configuration is the lowest among the three phosphor configurations, which indicates that in the same phosphor mass condition, the YCC phosphor configuration can make the phosphor more efficient. The results of the normalized intensity are different from the CCT distributions. The conventional phosphor configuration LED shows the best uniformity of intensity, while the YCC configuration performs the worst intensity distribution. However, the differences between the normalized intensities of the three phosphor configurations are within 10% of each other, which is low enough that can be ignored for practical application. The full angle at half maximum (FAHM) for all of the three configurations is around 120°, which is a typical value for such a secondary optical design.

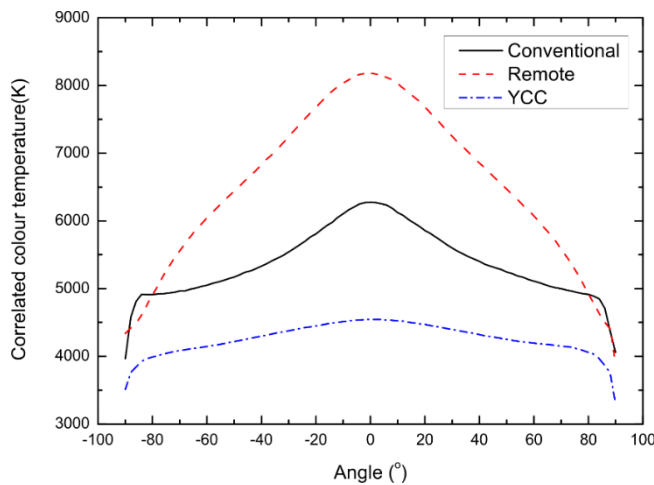


Fig. 9. The correlated color temperature distributions of different types of multi-chip LEDs

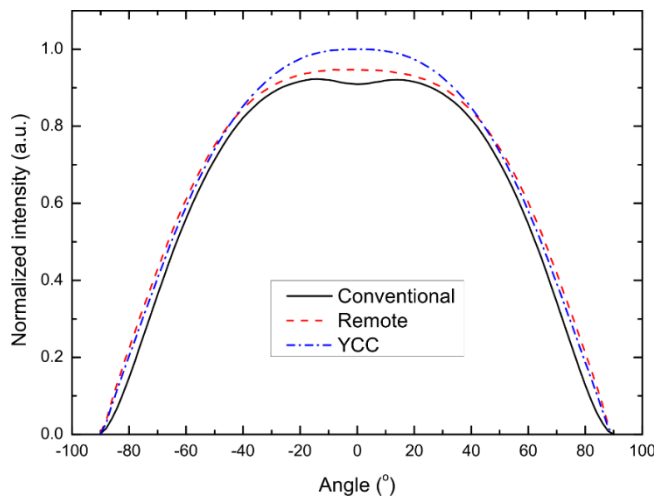


Fig. 10. The normalized intensity distributions of different types of multi-chip LEDs

4. Conclusions

In this work, a patterned phosphor configuration for high power multi-chip LEDs were proposed by a pulsing spray process, which improves the chromatic and luminous performance. The parameters of the patterned phosphor configurations were experimentally investigated and optimized. The results showed that the yellow central coating (YCC) configuration produced outstanding performance not only in chromatic uniformity but also in luminous. In comparison with the conventional phosphor coating, the YCC patterned phosphor LED can improve the luminous flux by 20.6%, and decrease the difference of the CCT distribution from 1362K to 489K. The YCC configuration is also capable of decreasing the average CCT value compared to other phosphor configurations in the same phosphor mass condition, which means that the YCC phosphor configuration is conducive to convert short wavelength light down to long wavelength light. Through this study, we believe that the application of the patterned phosphor configurations can enhance the optical properties of multi-chip LEDs.

Fundings

National Natural Science Foundation of China (51735004, 51775199); Natural Science Foundation of Guangdong Province (2014A030312017); Science & Technology Program of Guangdong Province (2015B010132005).